

Article

A Membrane Modified with Nitrogen-Doped TiO₂/Graphene Oxide for Improved Photocatalytic Performance

Tingting Li, Yong Gao *, Junwo Zhou, Manying Zhang , Xiaofei Fu and Fang Liu

School of Chemical and Environmental Engineering, Jiangsu University of Technology, Changzhou 213001, China; 13861046139@163.com (T.L.); 13775185565@163.com (J.Z.); myzhang@just.edu.cn (M.Z.); fuxiaofei@just.edu.cn (X.F.); liuf1213@just.edu.cn (F.L.)

* Correspondence: gaoyong@jsut.edu.cn; Tel.: +861340-155-8684

Received: 28 January 2019; Accepted: 24 February 2019; Published: 27 February 2019



Abstract: An improved photocatalytic microfiltration membrane was successfully prepared by the impregnation method with nitrogen-doped TiO₂/graphene oxide (GO) (NTG). By utilizing the unique role of N and GO, the photocatalytic activity of the membrane in UV and sunlight was improved. Compared with the Polyvinylidene Fluoride (PVDF) microfiltration membrane which was modified by TiO₂, N-TiO₂ (NT) and TiO₂-GO (TG), the NTG/PVDF membrane exhibited high photocatalytic efficiency and significantly improved photodegradation power to the methylene blue (MB) solution under ultraviolet light and sunlight, with the photocatalytic efficiency reaching 86.5% and 80.6%, respectively. Scanning electron microscopy (SEM), X-ray diffractometry (XRD) and Fourier transform infrared spectroscopy (FT-IR) were used to analyze the morphology, crystal structure and chemical bonds of the membrane surface. The hydrophilicity of the modified PVDF microfiltration membrane was significantly improved, the flux of the pure water membrane reached 1672 Lm⁻²h⁻¹, the flux of the MB solution was also significantly improved due to photodegradation. Therefore, the nitrogen-doped titanium dioxide graphene oxide PVDF microfiltration membrane (NTG/PVDF membrane) has great development prospects in sustainable water treatment.

Keywords: nitrogen-doped TiO₂; graphene oxide; photocatalysis; surface modification; microfiltration membrane

1. Introduction

Membrane separation is a promising separation and purification technology for pollutants. It is efficient and convenient [1]. However, during the treatment of wastewater by membrane separation, some problems had to be faced, such as low water flux, low rejection and poor contamination resistance. Photocatalysis is considered to be a low-cost and sustainable method to decompose organic pollutants, which can directly convert organic pollutants into inorganic small molecules such as H₂O and CO₂. However, there are some problems, such as catalyst separation, and so forth. In this case, the photocatalytic-membrane coupling membrane separation and photocatalysis can not only maintain the original advantages of the photocatalytic and membrane separation technology, but also solves and alleviates the problems that restrict the development of the two technologies [2–4].

Among the many photocatalysts, the TiO₂ photocatalyst is widely used in the field of water treatment because of its advantages of being cheap, being non-toxic, having strong photochemical stability and not causing secondary pollution [5,6]. The incorporation of TiO₂ nanoparticles into water filtration membranes enhances their flux, contaminant removal and contamination resistance [7]. However, a photocatalytic membrane made of TiO₂ alone has a very low photocatalytic performance under sunlight [8]. This problem has seriously hindered the widespread use of TiO₂ as a photocatalyst.

At present, the modification methods of TiO_2 include metal doping, non-metal doping, dye sensitization and semiconductor recombination. Nitrogen-doped TiO_2 is a non-metal modification. Nitrogen, instead of oxygen vacancies, introduces nitrogen into the TiO_2 gap, which effectively reduces the energy gap between the valence and the conduction band, significantly improving the photocatalytic activity of TiO_2 [9–11]. The excellent electron transfer properties of GO are considered to be ideal for expanding the photoresponse range of TiO_2 [12]. GO can be used as an electron transporter for TiO_2 nanoparticles so that the lifetime of electron-hole pairs can be significantly improved [13]. In addition, functional groups such as a carboxyl group and a hydroxyl group in GO can improve the hydrophilicity when used as an additive [14].

PVDF is an ideal membrane separation material due to its good thermal and chemical stability. However, the hydrophobicity of PVDF materials makes it easy to adsorb and deposit contaminants during application, causing membrane fouling and reducing the membrane life [15]. Therefore, it is usually necessary to hydrophilically modify PVDF. There are two main modification technologies for PVDF microfiltration membranes. One is the modification of the membrane body and the other is the modification of the membrane surface. Bulk modification is the modification of the raw material before membrane formation by blending. Surface modification is modification by implanting a hydrophilic group on the surface of the membrane. The bulk modification method has a limited hydrophilic effect, it makes it difficult to disperse the modifier, has a low photocatalytic activity and causes the physical-chemical properties to be prone to change. The surface modification hydrophilic effect is a significant improvement from this as it does not affect the physical-chemical properties of the membrane body and the modified membrane exhibits excellent photocatalytic properties [16]. There have been many studies on nitrogen-doped TiO_2/GO composite photocatalysts, the photocatalytic performance was remarkable but it was difficult to recycle the photocatalysts. In some research, the surface modification of the ultrafiltration membrane by TiO_2/GO was discussed and the results showed that the photodegradation performance of the modified membrane was improved but that the modification process was slightly complicated [3,17].

In this paper, the PVDF microfiltration membrane was modified by the surface coating method with nitrogen-doped TiO_2/GO composites. The morphology, crystal structure, hydrophilicity, surface functional groups, membrane flux, photodegradation kinetics and the effects of different light conditions on the degradation of photocatalytic membranes were analyzed.

2. Experimental

2.1. Materials

Graphite powder was purchased from Tanfeng graphene Technology Co. Ltd., Suzhou, China (www.graphenechina.com); the PVDF (0.22 μm) microfiltration membrane was purchased from Green League Chemical Co. Ltd., Jiangsu, China (www.gmhplc.com); Methylene blue (MB) was purchased from Zhanyun Chemical Co. Ltd., Shanghai, China (www.shzychem.com); Tetrabutyl titanate (AR) was purchased from Macklin Chemical Co. Ltd., Shanghai, China (macklin.company.lookchem.cn); anhydrous ethanol (AR), acetic acid (AR), concentrated sulfuric acid (98%, AR), potassium permanganate (99%, AR), hydrogen peroxide (AR), sodium hydroxide(AR), and urea (AR) was purchased from Qiangsheng Functional Chemical Co. Ltd., Jiangsu, China (www.qschem.com); sodium hydrogen sulfite(AR), and cetyltrimethylammonium bromide (CTBA)(AR) was purchased from Lingfeng Chemical Co. Ltd., Shanghai, China (lingfengshiji.foodmate.net).

2.2. Preparation of Nanomaterials

GO nanosheets were synthesized by the graphite-modified Hummers method [18].

Nitrogen-doped TiO_2 (NT) nanoparticles were prepared by sol-gel method and high-temperature calcination. First, 10 mL of tetrabutyl titanate was added to 20 mL of absolute ethanol to form Solution A. Solution B was a mixture of 10 mL of absolute ethanol, 15 mL of deionized water and 4.5 mL of

acetic acid, added to 0.01 g urea. After adjusting the pH of solution B to 2–3 with HCl aq., solution B was slowly added dropwise to solution A under vigorous stirring. A mixed solution was obtained after the completion of the titration and stirring was continued for about 1 h under the action of a magnetic stirrer. Then it was aged for 2 h to form a yellow transparent gel. The mixture was dried in an oven at 100 °C and yellow crystals formed. The solid was converted into a white powder by grinding. It was then calcined at 500 °C for 2 h to complete the preparation of NT. The preparation of TiO₂ was the same as in the above case, except urea was not added.

Nitrogen-doped TiO₂/GO (NTG) was prepared by a hydrothermal method. First, 0.05 g of GO was dispersed in 80 mL of deionized water and sonicated for 1 h. An additional 1 g of NT was added and a further 1 h sonication was required. Then the blend suspension was transferred to a 100 mL Teflon-lined stainless steel autoclave, which was kept at 180 °C for 18 h, and cooled to room temperature. Finally, the suspension was centrifuged at 5000 rpm, then washed with deionized water three times, and dried under a vacuum at 60 °C. TG was prepared by the same method but without urea.

2.3. Modification of the PVDF Microfiltration Membrane

The PVDF microfiltration membrane was immersed in deionized water for 0.5 h, then the membrane was immersed in the prepared KMnO₄ (3%) and NaOH (3 mol/L) solution. The membrane was washed out by deionized water because it turned yellowish brown and it placed in a solution of NaHSO₃ (2%) to a nucleophilic reaction until the yellowish-brown color was completely removed. The membrane was taken out and washed with deionized water until neutral, then it was immersed in an appropriate amount of surfactant CTAB (1 g/L) solution for 5 min.

A total of 0.1 g prepared NTG nanopowder was dispersed by sonication in 100 mL of deionized water for 1 h to form a suspension. The treated PVDF membrane was placed in the suspension, incubated at 80 °C for 3 h, taken out to be washed and dried, and then the NTG/PVDF microfiltration membrane was prepared. The preparation of TiO₂/PVDF, NT/PVDF, TG/PVDF was the same as the above process. The loadings of the four membranes (TiO₂/PVDF, NT/PVDF, TG/PVDF, NTG/PVDF) were 0.0221, 0.0216, 0.0187, and 0.0332 g, respectively.

2.4. Modified Membrane Characterization

The surface morphology of the modified membrane was characterized by scanning electron microscopy (SEM) (Carl Zeiss AG, Oberkochen, Germany, www.zeiss.com.cn). The crystal structure of the nanoparticles on the surface of the modified membrane was determined by X-ray diffractometry (XRD) (Bruker, Santa Barbara, CA, USA, www.bruker.com). The chemical bonds on the surface of the membrane were characterized by Fourier transform infrared spectroscopy (FT-IR) (Thermo Scientific, Waltham, MA, USA, www.thermofisher.com). The hydrophilicity of the membrane surface was investigated by water contact angle meter (Micaren, Xiamen, China, www.micaren.com).

2.5. Modified Membrane Performance Tests

The pure water flux (J_w) of the prepared membrane and the flux of the methylene blue (MB) solution (J_0 and J were the flux before and after the reaction) were determined in Figure 1 by a self-made flux measuring device. The upper side of the device was made of quartz glass to facilitate irradiation through ultraviolet light and visible light during filtration. The feed tank was pressurized with a nitrogen bottle and a PVDF microfiltration flat membrane (diameter 50 mm, pore diameter 220 nm) was placed in the center of the device. The water flux was monitored by a digital balance and the data were automatically recorded and analyzed by the acquisition software. Before testing the pure water flux, to get stable pure water flux, the deionized water was filtered at a 0.2 MPa pressure at room temperature for 1 h, then the pressure was adjusted to 0.1 MPa. The data were periodically recorded using a digital balance equipped with a computer. Thereafter, the MB solution was used instead of pure water as a feed solution to test the flux of the MB solution.

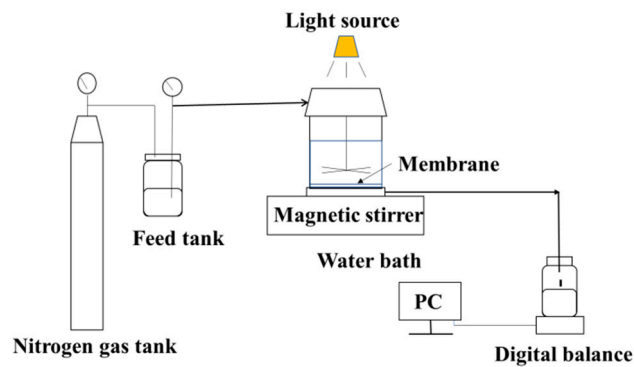


Figure 1. The laboratory self-made flux measurement device diagram.

The photocatalytic performance of the modified membranes was evaluated by decomposing MB (50 mg/L) in the self-made apparatus (shown in Figure 2) in a dark/ultraviolet/sunlight environment. The membrane was fixed on a frame and immersed in a reactor containing the MB solution. The UV source was a 120-watt built-in ballast UV lamp and the sunlight source was a 100-watt xenon lamp. The absorbance of the MB solution treated under different light sources was measured using an ultraviolet spectrophotometer (UV, Purkinje, Beijing, China, www.pgeneral.com) at a measuring wavelength of 664 nm.

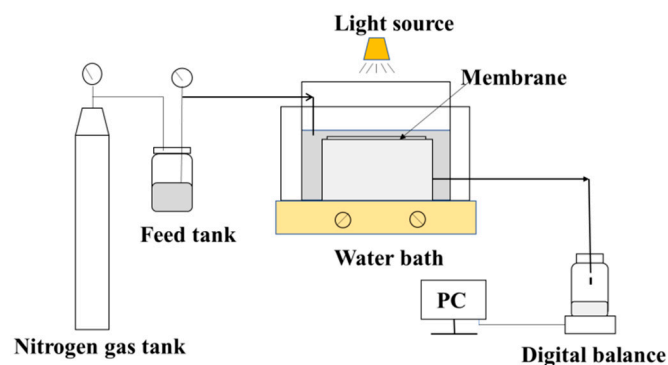


Figure 2. The laboratory self-made methylene blue degradation device.

3. Results and Discussion

3.1. Modified Membrane Morphology

In order to evaluate the modified membrane morphology, SEM was used to observe the surface topography of the PVDF, TiO₂/PVDF, NT/PVDF, TG /PVDF and NTG/PVDF membranes. It was observed (Figure 3) that the surface portion of the TiO₂ modified membrane was covered by TiO₂ nanoparticles and some of the darker regions still showed the exposed surface of PVDF. In contrast, the NT modified membrane had a large amount of nanoparticle aggregation on the surface and the fabric-like features produced by the GO nanosheet could be observed clearly on the TG membrane. The surface loading of the NTG membrane was more complete and uniform and the NT forms a good distribution on the GO sheet, thereby increasing the surface area and photocatalytic performance of the NTG membrane.

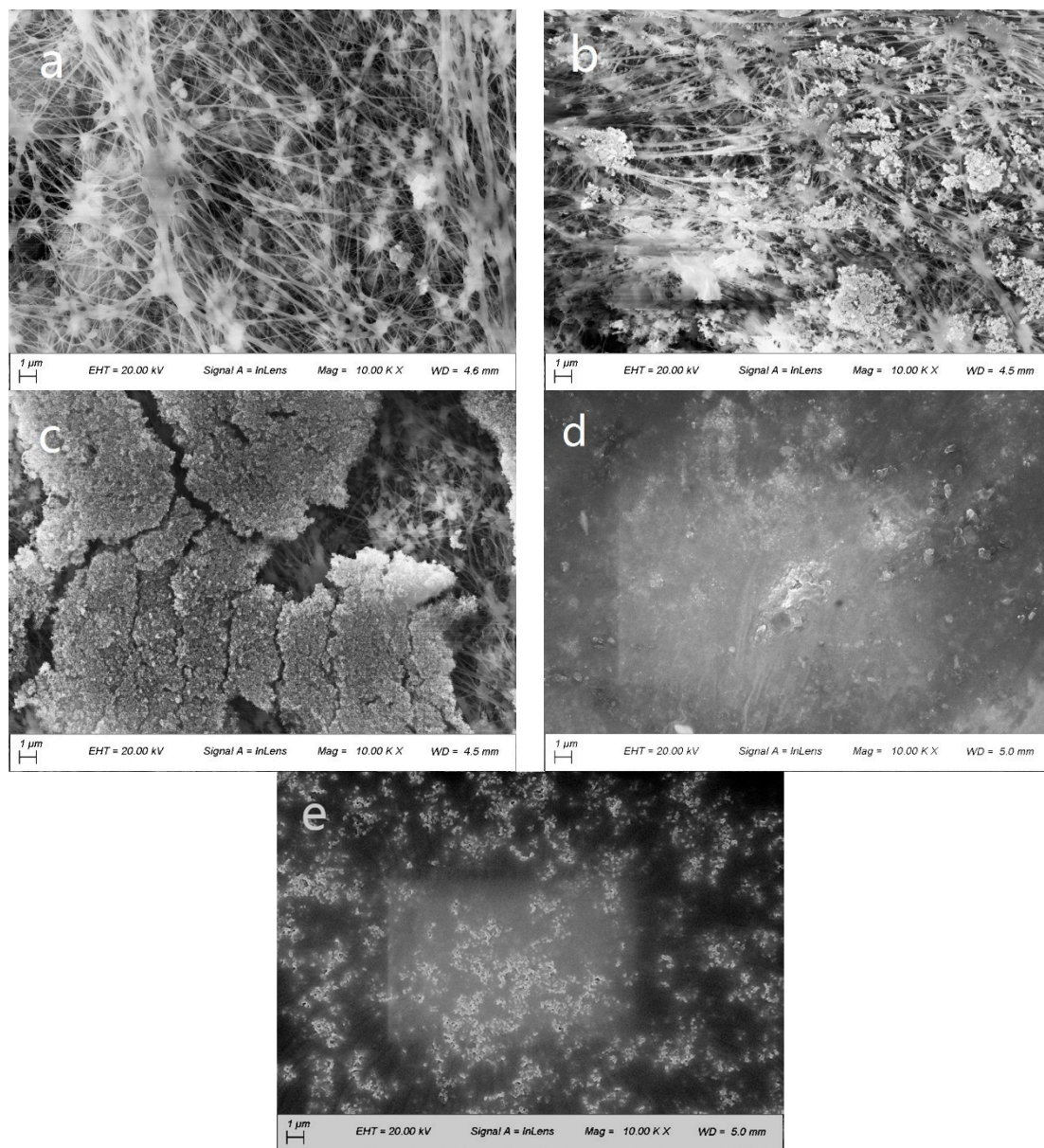


Figure 3. Scanning electron microscopy (SEM) image of the modified membrane surface: (a) Polyvinylidene Fluoride (PVDF) membrane; (b) TiO_2 /PVDF membrane; (c) nitrogen-doped TiO_2 (NT)/PVDF membrane; (d) TiO_2 -graphene oxide (TG)/PVDF membrane and (e) nitrogen-doped TiO_2 /graphene oxide NTG/PVDF membrane.

3.2. The X-Ray Diffraction Analysis of Modified Membrane

Figure 4A was an XRD spectrum of graphite oxide, in which a characteristic peak corresponding to the (001) plane of the graphite oxide layered structure appears in the vicinity of $2\theta = 10^\circ$ and the (002) plane characteristic peak of graphite disappears, which indicated that most of the graphite had been oxidized. The XRD pattern of the PVDF microfiltration membrane modified by different photocatalysts was shown in Figure 4B. The four catalysts supported on the surface were mainly of the anatase TiO_2 crystal structure; 2θ was equal to 25.3 (101), 37.9 (004), 48.1 (200), 54 (105, 211), 62.7 (204), 69.1 (116, 220), and 75 (215). The doping of N and GO had no significant effect on the crystal structure of nano-titanium dioxide. There was no characteristic diffraction peak of graphite oxide in Figure 4B, which may have been due to the orderly layering of graphite oxide due to the ultrasonic dispersion and subsequent hydrothermal treatment. The structure was destroyed and partially reduced graphene

oxide was formed, TiO_2 particles were formed on the surface of the graphene oxide sheet layer, which hinders the ordered packing of the graphene oxide layer sheet.

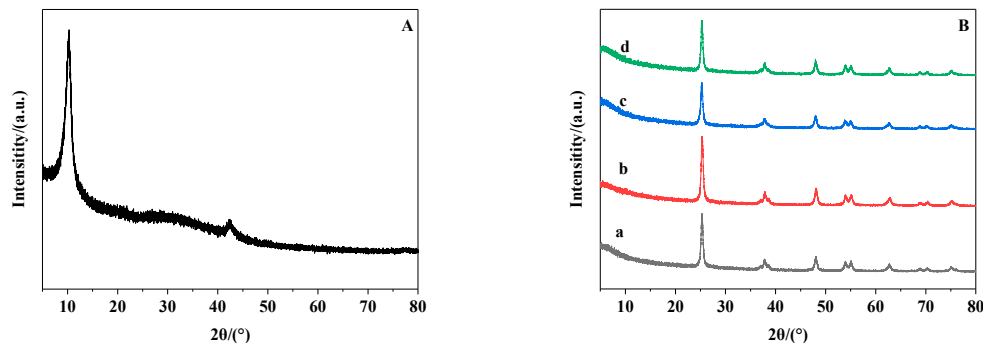


Figure 4. The x-ray diffractometry (XRD) spectra of (A) graphene oxide and (B): (a) TiO_2 /PVDF membrane; (b) NT/PVDF membrane; (c) TG/PVDF membrane and (d) NTG/PVDF membrane.

3.3. The Water Contact Angle of the Modified Membrane

The rougher surface of a membrane results in a higher contact angle. The roughness of the modified membrane increased was observed to have increased by eye and SEM observations (shown in Figure 3). However, this effect of the increase of the roughness of the modified membrane on the hydrophilicity was smaller than the increase of the hydrophilic property of the membrane modified by the NGT catalyst. Therefore, the contact angle value decreased (shown in Figure 5). The water contact angle of the pure PVDF membrane was 96.5° . During the phase inversion in the modification process of the membranes, due to the presence of hydrophilic oxygen-containing functional groups, the nanomaterial rapidly migrated to the surface of the membrane, forming a tight hydration layer, which affected the contact angle of the modified membrane [19–21]. With the addition of nanomaterials, the contact angle of the modified membranes gradually decreased and the contact angle of the NTG/PVDF membrane dropped to 45.6° due to the hydrophilicity of the nanomaterial. Compared with the other membranes, the NTG/PVDF membrane had the lowest water contact angle, which was mainly related to the higher affinity of GO and TiO_2 for water and the hydrolysis of hydroxyl groups. The interface between GO nanosheets and NT nanoparticles was more uniform. This resulted in a more uniform dispersion of NT on the GO surface [22], which improved the hydrophilicity of the NTG/PVDF membrane.

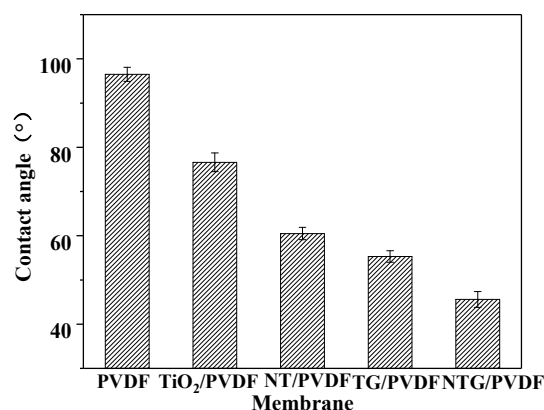


Figure 5. The water contact angle of the membrane.

3.4. The Infrared Spectroscopy Analysis of the Modified Membranes

Figure 6 is the infrared spectrum of the PVDF membrane and the NTG/PVDF membrane. It can be seen that a large number of polar groups such as $-\text{OH}$, $\text{C}-\text{O}$ and $\text{C}=\text{O}$ were introduced on the surface of the modified membranes, which significantly improved the hydrophilicity of the modified

membranes. A broad absorption peak appearing at 3294 cm^{-1} , corresponded to the stretching vibration absorption peak of -OH . The vicinity of 2900 cm^{-1} corresponded to the vibration absorption peak of -CH_2 , 1712 cm^{-1} corresponded to the vibration absorption peak of C=O , 1399 cm^{-1} was attributed to the deformation vibration of C-OH , 1241 cm^{-1} corresponded to the stretching vibration peak of C-O in C-OH , and 1017 cm^{-1} was the stretching vibration peak of C-O in C-O-C [23]. The stretching vibration of C-N at about 1050 cm^{-1} showed that the modified membrane was doped with nitrogen and the peak at $400\text{--}600\text{ cm}^{-1}$ was the stretching vibration of Ti-O-Ti .

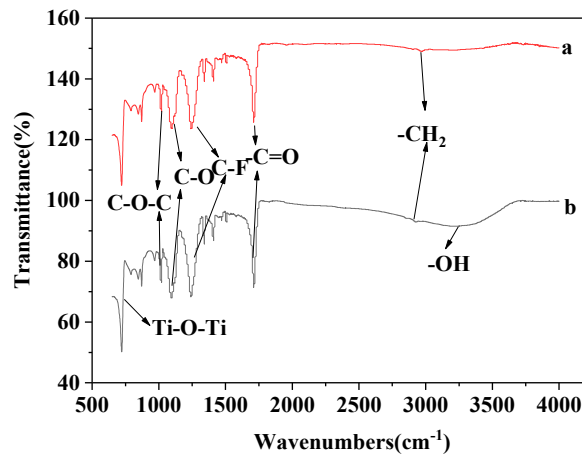


Figure 6. The infrared spectroscopy analysis of the (a) PVDF membrane and the (b) NTG/PVDF membrane.

3.5. The Flux Change Analysis of the Modified Membrane

The pure water membrane flux was obtained by the experimental self-made flux device. As shown in Figure 7, the pure water flux of the PVDF membrane was $530\text{ Lm}^{-2}\text{h}^{-1}$ and the pure water flux of the NTG/PVDF membrane reached $1672\text{ Lm}^{-2}\text{h}^{-1}$. Compared to the PVDF membrane, the pure water flux of the NTG/PVDF membrane increased by 3.15 times because the doping of nitrogen and GO increased the hydrophilicity of the TiO_2 . The composite microfiltration membranes were prepared by the surface coating method. The photocatalysts were attached to the surface of the membranes in a dispersed state and no nanoparticle adhesion was observed inside the pores of the membranes because the specific surface area in the pore size was large and the surface tension of the membrane was also relatively large. Therefore, the nanoparticles could not enter the pores and few nanoparticles adhered in the pores of the membrane.

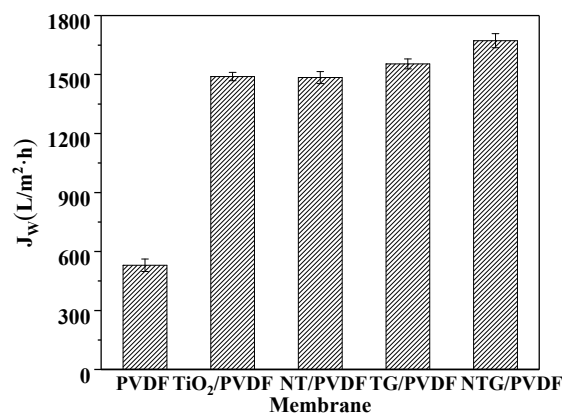


Figure 7. The pure water flux of the membrane.

The MB solution flux of the modified microfiltration membrane was tested under dark, ultraviolet and sunlight conditions. The relative flux changed, as shown in Figure 8a. In the dark, a sharp drop in

pure PVDF membrane was observed during MB filtration. As shown in Figure 8b, the MB solution flux of all the membranes under ultraviolet light was significantly improved when compared to the darkness condition since the photodegradation of the MB inhibited membrane fouling during the filtration process. In particular, the NTG/PVDF membrane flux had a maximal increase, which was consistent with its excellent photocatalytic activity and hydrophilicity. The MB solution flux of all membranes in sunlight was shown in Figure 8c. Due to the slightly poor photocatalytic effect in sunlight, the TiO₂/PVDF membrane and the NT/PVDF membrane showed only a slight flux increase compared to their performance in the dark. The relative flux of the NTG/PVDF membrane and TG/PVDF also decreased slowly. The penetration effect of the NTG/PVDF membrane on the MB was slightly better because the photocatalytic activity of the NTG/PVDF membrane was stronger than that of the TG/PVDF membrane. In addition, pure PVDF membranes showed similar flux declines in the dark, as well as in ultraviolet light and sunlight, due to membrane fouling, indicating that pure PVDF membranes have little photocatalytic activity under ultraviolet light and sunlight.

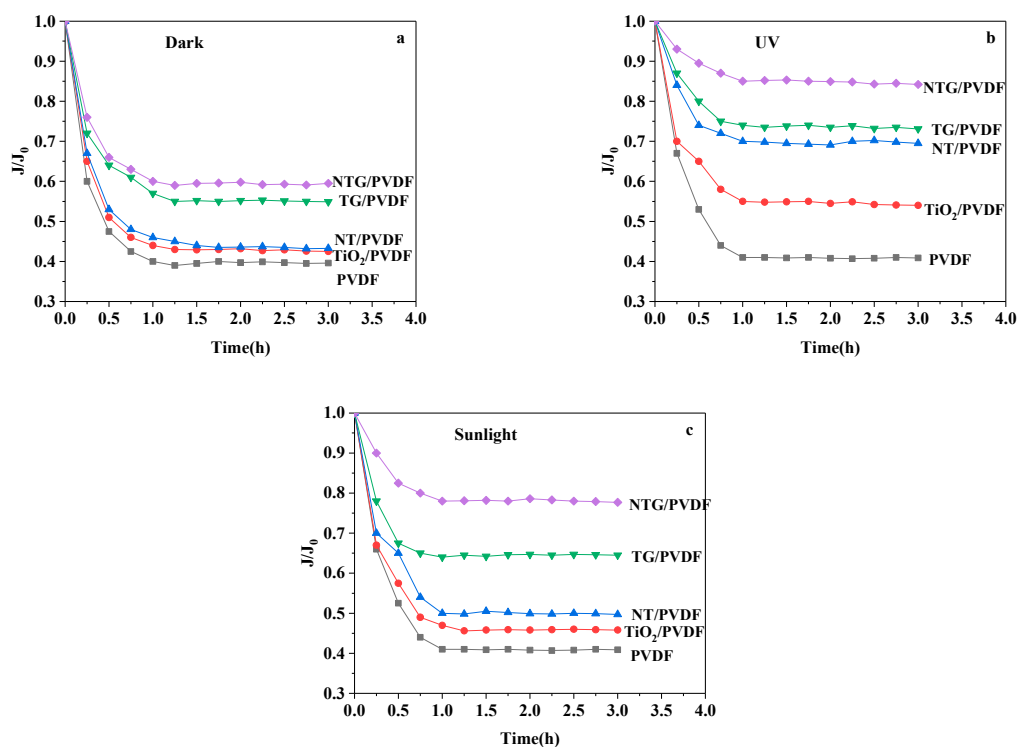


Figure 8. The relative flux of the methylene blue (MB) solution (a) in the dark; (b) ultraviolet and (c) sunlight conditions.

3.6. The Photocatalytic Degradation Properties of the Modified Membranes

The photocatalytic activity of the PVDF, TiO₂/PVDF, NT/PVDF, TG/PVDF, NTG/PVDF membranes was evaluated by the degradation of MB under darkness and ultraviolet/sunlight illumination. Figure 9a shows that when the adsorption capacity of the membranes was measured in the dark, all membranes had almost the same adsorption capacity for MB, while the TG/PVDF and NTG/PVDF membranes had a slightly higher adsorption capacity due to the participation of GO. The GO structure provided a high specific surface area, resulting in good adsorption properties. However, the number of GO and TiO₂ nanoparticles supported on the surface of the membrane was small so there was no significant influence on the removal of the MB solution by adsorption. The PVDF membrane had a very low MB removal rate under ultraviolet light and sunlight, indicating that the PVDF membrane itself had almost no photocatalytic performance. After modification by nanomaterials, the membranes exhibited an enhanced photocatalytic activity under ultraviolet light, but when exposed to sunlight, the TiO₂/PVDF membrane only showed a slight MB degradation

compared to the NT/PVDF, TG/PVDF and NTG/PVDF membranes. This was because TiO_2 could only be photocatalyzed by ultraviolet irradiation. Compared to the TiO_2 /PVDF membranes, the NT/PVDF and TG/PVDF membranes exhibited higher photocatalytic efficiency because nitrogen doping significantly increased the absorption of visible light in the photocatalysts and the high charge mobility of the GO nanosheets was beneficial to the Electron transfer and separation. Compared to the NT/PVDF and TG/PVDF membranes, the NTG/PVDF membranes had higher photocatalytic activity under ultraviolet light and sunlight, with MB degradation rates reaching 86.5% and 80.6%, respectively. The addition of GO could act as a semiconductor photosensitizer, shifting the Fermi level of the catalyst in the positive direction and enhancing the absorption of visible light. Due to the excellent electrical conductivity of GO, electrons were transported at a high speed, reducing the recombination rate of the electrons and holes [17]. The effect of N doping on the activity of the catalyst significantly improved with the addition of GO. This was because the doping of N significantly reduced the forbidden bandwidth of the catalyst and enhanced its response to visible light.

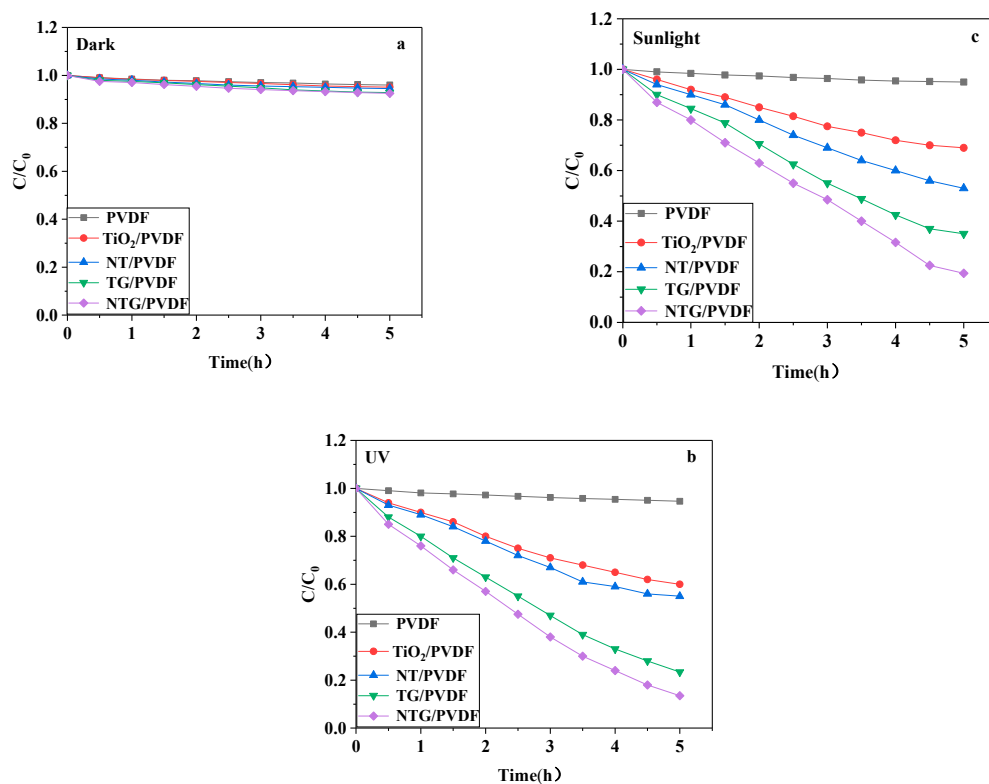


Figure 9. The photodegradation of MB by the membranes in (a) darkness (b) under ultraviolet light and (c) under sunlight.

3.7. The Kinetic Analysis of the Photocatalytic Degradation of the Modified Membranes

In order to quantify the effect of various modifications on the photocatalytic activity of the membrane, the first-order reaction kinetic equation $\ln(C/C_0) = -kt$ was used to fit the kinetics of MB degradation into the various surface-modified membranes (where C and C_0 are the MB concentrations during the experiment and at the beginning of the experiment, respectively; k is the reaction rate constant, and t is the reaction time). The process of MB degradation by the modified membranes with different photocatalysts was consistent with first-order kinetics. Figure 10 summarizes the photodegradation dynamic curves of the TiO_2 /PVDF, NT/PVDF, TG/PVDF, and NTG/PVDF membranes under UV and sunlight, respectively. Under UV light, the degradation rate constants of the NTG/PVDF and TG/PVDF membranes were significantly higher than those of the TiO_2 /PVDF and NT/PVDF membranes (shown in Figure 10a). This is due to the synergy between GO and TiO_2 . Graphene has a very high electron transport rate, which can accelerate the photogenerated electron

transfer rate of TiO_2 after compounding it with GO, thereby improving the photocatalytic activity of the composite catalyst [24].

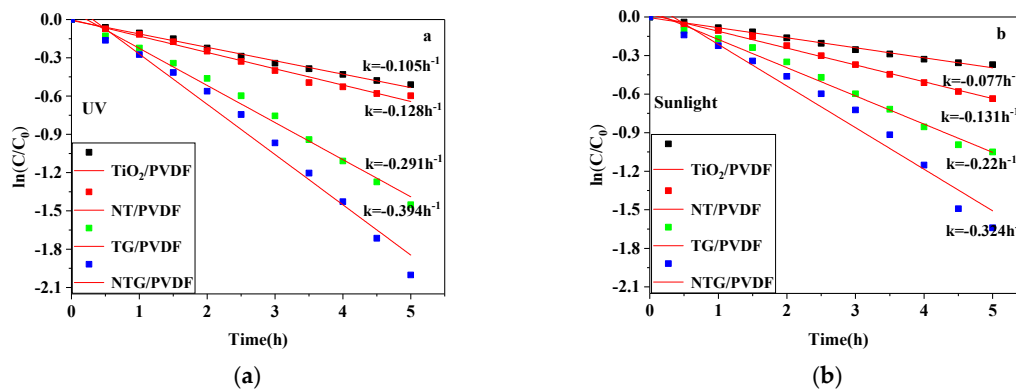


Figure 10. The MB photodegradation kinetics curves under (a) ultraviolet light and (b) sunlight.

Figure 10b showed that the combination of N, GO and TiO_2 clearly produced a significant synergistic effect in sunlight. The MB photodegradation rate constants of the NTG/PVDF, TG/PVDF, NT/PVDF membranes were significantly higher than the TiO_2 /PVDF membranes. This is because N-doping improves the visible light absorption of TiO_2 . The effect of GO can be further improved by N-doping. The electron-hole recombination in TiO_2 can be effectively reduced, thereby significantly improving the photocatalytic performance of the NTG microfiltration membranes.

The NTG/PVDF membranes and TG/PVDF membranes had very similar photocatalytic properties under UV, while the NTG/PVDF membrane performed better in sunlight than the TG/PVDF membranes, indicating that N-doping has no significant effect on UV light. However, this is not the case in sunlight. Nitrogen doping reduced the forbidden bandwidth of TiO_2 . Thus, TiO_2 had a longer photoresponse range.

4. Conclusions

This experiment was mainly aimed at the preparation and photodegradation performance of the modified photocatalytic composite membranes. The PVDF microfiltration membrane was modified by the surface coating method with different photocatalysts: TiO_2 /PVDF, NT/PVDF, TG/PVDF, and NTG/PVDF, respectively. The properties of the modified membranes were characterized by SEM, XRD, FT-IR and a water contact angle meter, and the effects of the different photocatalysts on the photocatalytic activity of the modified membranes were investigated. The results showed that the surface loading of the NTG/PVDF membrane was more complete and uniform and that the doping of N and GO had no significant effect on the crystal structure of nano-titanium dioxide, mainly an anatase crystal structure. The hydrophilic functional groups on the surface of the modified membranes were increased and the hydrophilicity was remarkably improved. The pure water flux of the NTG/PVDF membrane was the best due to the increased hydrophilicity of NTG, the relative flux of the MB solution was also improved by photodegradation under different illumination conditions. The NTG/PVDF membrane showed the best photodegradation performance with degradation rates reaching 86.5% and 80.6% under ultraviolet and sunlight, respectively. Therefore, the NTG/PVDF membranes have great development prospects in sustainable water treatment.

Author Contributions: Conceptualization—T.L. and Y.G.; Data curation—T.L.; Formal analysis—Y.G.; Funding acquisition—M.Z. and Y.G.; Investigation—T.L., Y.G. and J.Z.; Methodology—T.L.; Writing, original draft—T.L.; Writing, review & editing—Y.G., X.F. and F.L.

Funding: This research was funded by National Science Foundation Natural Fund, grant number 51508239.

Acknowledgments: This work was supported by the National Science Foundation Natural Fund (NO.51508239), Jiangsu Province Industry-University Research Prospective Joint Research Project (NO. BY2016030-26), A Project Funded by Jiangsu Postgraduate Practice Innovation (NO. SJCX18-0989 and NO. SJCX18-1011).

Conflicts of Interest: The authors declare no conflict of interest.

References

1. Buonomenna, M.G. Membrane processes for a sustainable industrial growth. *RSC Adv.* **2013**, *3*, 5694–5740. [[CrossRef](#)]
2. Zhang, H.F.; Wang, J.Y. Catalytic Separation Membrane in Water Treatment. *Bull. Chin. Ceram. Soc.* **2016**, *35*, 1130–1136.
3. Gao, Y.; Hu, M.; Mi, B. Membrane surface modification with TiO₂–graphene oxide for enhanced photocatalytic performance. *J. Membrane Sci.* **2014**, *455*, 49–356. [[CrossRef](#)]
4. Chong, M.N.; Jin, B.; Chow, C.W.; Saint, C. Recent developments in photocatalytic water treatment technology: a review. *Water Res.* **2010**, *44*, 2997–3027. [[CrossRef](#)] [[PubMed](#)]
5. Liu, G.; Han, C.; Pelaez, M.; Zu, D. Enhanced visible light photocatalytic activity of C N-codoped TiO₂ films for the degradation of microcystin-LR. *J. Mol. Catal. A: Chem.* **2013**, *372*, 58–65. [[CrossRef](#)]
6. Liu, G.; Han, C.; Pelaez, M.; Zhu, D.; Liao, S.; Likodimos, V.; Ioannidis, N.; Kontos, A.G.; Falaras, P.; Dunlop, P.S. Synthesis, characterization and photocatalytic evaluation of visible light activated C-doped TiO₂ nanoparticles. *Nanotechnology* **2012**, *23*, 294003. [[CrossRef](#)] [[PubMed](#)]
7. Romanos, G.E.; Athanasekou, C.P.; Katsaros, F.K.; Kanellopoulos, N.K.; Dionysiou, D.D.; Likodimos, V.; Falaras, P. Double-side active TiO₂-modified nanofiltration membranes in continuous flow photocatalytic reactors for effective water purification. *J. Hazard. Mater.* **2003**, *99*, 304–316. [[CrossRef](#)] [[PubMed](#)]
8. Almeida, N.A.; Martins, P.M.; Teixeira, S.; Lopes da Silva, H.A.; Sencadas, V.; Kühn, K.; Cuniberti, G.; Lanceros-Mendez, S.; Marqueset, P.A.A.P. TiO₂/graphene oxide immobilized in (PVDF-TrFE) electrospun membranes with enhanced visible-light-induced photocatalytic performance. *J. Mater. Sci.* **2016**, *51*, 6974–6986. [[CrossRef](#)]
9. Sher Shah, M.S.; Kim, W.J.; Park, J.; Rhee, D.K.; Jang, I.-H.; Park, N.-G.; Lee, J.Y.; Yoo, P.J. Highly Efficient and Recyclable Nanocomplexed Photocatalysts of AgBr/N-Doped and Amine-Functionalized Reduced Graphene Oxide. *ACS Appl. Mater. Interfaces* **2014**, *6*, 20819–27. [[CrossRef](#)] [[PubMed](#)]
10. Chen, D.; Zou, L.; Li, S.; Zheng, F. Nanospherical like reduced graphene oxide decorated TiO₂ nanoparticles: an advanced catalyst for the hydrogen evolution reaction. *Sci. Rep.* **2016**, *6*, 20335. [[CrossRef](#)] [[PubMed](#)]
11. Mou, Z.; Wu, Y.; Sun, J.; Yang, P.; Du, Y.; Lu, C. TiO₂ nanoparticles-functionalized N-doped graphene with superior interfacial contact and enhanced charge separation for photocatalytic hydrogen generation. *ACS Appl. Mater. Interfaces* **2014**, *6*, 13798–13806. [[CrossRef](#)] [[PubMed](#)]
12. Atchudan, R.; Edison, T.N.J.I.; Perumal, S.; Karthikeyan, D.; Lee, Y.R. Effective photocatalytic degradation of anthropogenic dyes using graphene oxide grafting titanium dioxide nanoparticles under UV-light irradiation. *J. Photochem. Photobiol. A: Chem.* **2017**, *333*, 92–104. [[CrossRef](#)]
13. Zhang, Y.; Zhang, N.; Tang, Z.R.; Xu, Y.J. Improving the photocatalytic performance of graphene-TiO₂ nanocomposites via a combined strategy of decreasing defects of graphene and increasing interfacial contact. *Phys. Chem. Chem. Phys.* **2012**, *14*, 9167–9175. [[CrossRef](#)] [[PubMed](#)]
14. Kibechu, R.W.; Ndinteh, D.T.; Msagati, T.A.M.; Mamba, B.B.; Sampath, S. Effect of incorporating graphene oxide and surface imprinting on polysulfone membranes on flux, hydrophilicity and rejection of salt and polycyclic aromatic hydrocarbons from water. *Phys. Chem. Earth* **2017**, *100*, 126–134. [[CrossRef](#)]
15. Cao, X.; Ma, J.; Shi, X.; Ren, Z. Effect of TiO₂, nano particle size on the performance of PVDF membrane. *Appl. Surf. Sci.* **2006**, *253*, 2003–2010. [[CrossRef](#)]
16. Ye, T.; Chen, W.; Xu, H.; Geng, N.; Cai, Y. Preparation of TiO₂/graphene composite with appropriate N-doping ratio for humic acid removal. *J. Mater. Sci.* **2018**, *53*, 613–625. [[CrossRef](#)]
17. Safarpour, M.; Khataee, A.; Vatanpour, V. Thin film nanocomposite reverse osmosis membrane modified by reduced graphene oxide/TiO₂ with improved desalination performance. *J. Membrane Sci.* **2015**, *489*, 43–54. [[CrossRef](#)]
18. Marcano, D.C.; Kosynkin, D.V.; Berlin, J.M.; Sinititskii, A.; Sun, Z.; Slesarev, A.; Alemant, L.B.; Lu, W.; Tour, J.M. Improved synthesis of graphene oxide. *ACS Nano* **2010**, *4*, 4806–4814. [[CrossRef](#)] [[PubMed](#)]
19. Esfahani, M.R.; Tyler, J.L.; Stretz, H.A.; Wells, M.J.M. Effects of a dual nanofiller, nano-TiO₂ and MWCNT, for polysulfone-based nanocomposite membranes for water purification. *Desalination* **2015**, *372*, 47–56. [[CrossRef](#)]

20. Ganesh, B.M.; Isloor, A.M.; Ismail, A.F. Enhanced hydrophilicity and salt rejection study of graphene oxide-polysulfone mixed matrix membrane. *Desalination* **2013**, *313*, 199–207. [[CrossRef](#)]
21. Rabiee, H.; Vatanpour, V. Preparation and characterization of emulsion poly (vinyl chloride) (EPVC)/TiO₂ nanocomposite ultrafiltration membrane. *J. Membrane Sci.* **2014**, *472*, 185–193. [[CrossRef](#)]
22. Nie, C.; Ma, L.; Xia, Y.; He, C.; Deng, J.; Wang, L.; Cheng, C.; Sun, S.; Zhao, C. Novel heparin-mimicking polymer brush grafted carbon nanotube/PES composite membranes for safe and efficient blood purification. *J. Membrane Sci.* **2015**, *475*, 455–468. [[CrossRef](#)]
23. Li, D.M.; Jiang, P.; Ye, T.J.; Liang, J.L.; Li, S.X.; Jiang, S.X. Study on preparation conditions and antifouling properties of GO-TiO₂ modified PVDF hollow fiber membrane. *Acta Sci. Circum.* **2017**, *37*, 3746–3754.
24. Xu, H.; Ding, M.; Liu, S.; Li, Y.; Shen, Z.; Wang, K. Preparation and characterization of novel polysulphone hybrid ultrafiltration membranes blended with N-doped GO/TiO₂ nanocomposites. *Polymer* **2017**, *117*, 198–207. [[CrossRef](#)]



© 2019 by the authors. Licensee MDPI, Basel, Switzerland. This article is an open access article distributed under the terms and conditions of the Creative Commons Attribution (CC BY) license (<http://creativecommons.org/licenses/by/4.0/>).